J Mater Sci (2007) 42:7956–7963
DOI 10.1007/s10853-006-1287-x

Welding of aluminium by the MIG process with indirect electric arc (MIG-IEA)

R. García · V. H. López · E. Bedolla

Received: 30 March 2006 / Accepted: 16 November 2006 / Published online: 1 June 2007

Abstract A novel modification of the metal inert gas (MIG) welding method, which was developed to weld metal matrix composites, was applied to join plates of aluminium 12.5 mm thick. The plates were prepared with square edges and with a small single-V preparation with an angle of 45° in the upper part. The electric arc was indirectly applied on the single-V butt weld over strips of Al-2024 placed on top of the joint. Thermal analysis showed that the efficiency of the MIG process with indirect electric arc (IEA) is increased due to the reduction of heat losses and fully penetrated welds with a high depth-to-width ratio can be produced as compared to plain MIG welding in which partial penetration and lack of lateral fusion were observed. Microstructural examination of the welds revealed distinct characteristics such as partially melted grains trapped within the weld next to the fusion line for IEA welds and the typical epitaxial and columnar growth from the base metal partially melted grains for plain welds, i.e. direct application of the electric arc (DEA).

Introduction

The electric arc is the power source employed in most welding processes as heat source to accomplish fusion. The heat generated by an electric arc and hence the heat supplied to the area to be welded is effectively used and controlled to primarily achieve, the destruction of the oxide film of the metallic surfaces and subsequently the flow of weld metal over the melted faces to obtain a solution having both mechanical and chemical continuity as perfect as possible after solidifying [1]. During the fusion process, however, the heat generated by the electric arc cannot be fully used. The efficiency of the MIG welding process varies from 66% to 75%, with convection, conduction, radiation and splashes, the main sources of the losses [1–4].

The temperatures developed by the electric arc vary from 5,000 to 30,000 °C, depending on the plasma nature and the current conducted by the plasma [1]. Moreover, in the spray transfer mechanism, the liquid drops of Al detach at approximately 2,200 °C. It is thus established that the elevated temperatures developed by the electric arc produce weld pools with temperatures above 2,000 °C [5–7]. The temperature reached by the drops of metal transferred, the stick out and the impact of the drops over the weld pool have been modelled to establish the influence of these variables in the geometry of the weld pool and thereby in the welded joint [8, 9]. The results obtained from these studies are in broad agreement with the experimental configuration of the weld pool.

The direct establishment of the electric arc during the welding process of metallic materials gives rise to full exposure of the materials to the elevated temperatures developed by the process. Although all metallic materials can be joined by the MIG welding process, the penetration is not enough to weld in one pass a thickness of 12.5 mm in aluminium and therefore a multi-pass procedure is required giving rise to wide and non-uniform welds as a result of the significant volume of metal that has to be fed to fill the groove of the joint. Low dilution of the base metal with minimum weld defects and uniform cross weld profiles are features that can be obtained, although at high cost, by the

R. García (✉) · V. H. López · E. Bedolla
Instituto de Investigaciones Metalúrgicas, Universidad Michoacana de San Nicolás de Hidalgo,
A.P. 888, Morelia 58 000 Michoacán, México
e-mail: rgarcia@jupiter.umich.mx

high concentration energy welding processes such as laser or electron beam. This study seeks to test the feasibility of using the MIG indirect electric arc (IEA) technique, originally developed to weld metal matrix composites [10, 11], to weld thick sections of aluminium. The MIG-IEA welding process proposes to make good use of the thermal energy generated by the electric arc to succeed fusion and welding of thick aluminium plates in one welding pass.

Experimental procedure

Equipment, materials and welding details

A constant-current power source of 300 A with a voltage range of 0–50 V was employed. Weld beads were deposited using direct and indirect electric arc over the butt joints formed by two pure aluminium (Al-1010) plates. The design of the joints and their dimensions are shown in Fig. 1. The size of the Al plates was 12.5 mm × 40 mm × 200 mm. An electrode ER4043 of 1.2 mm in diameter with reverse polarity was employed. The metal at which the direct arc was applied to indirectly join the Al-1010 plates, was an Al-2024 alloy of 5 mm × 20 mm × 200 mm, the strips were used as feed metal placed over the butt joint of the Al-1010 plates forming a groove of 2 mm, as shown in Fig. 1b. An Al-2024 alloy was chosen as feeding material in the MIG-IEA process due to its fluidity in molten state. Pure argon was used as shield gas and pre-heating temperatures of 50 and 100 °C were investigated. Although pre-heating is not a recommended practice when welding Al or Al-alloys, it was found to be necessary for welding thick sections with the MIG-IEA method. The chemical compositions of the metallic materials employed and welding parameters are shown in Tables 1 and 2, respectively.

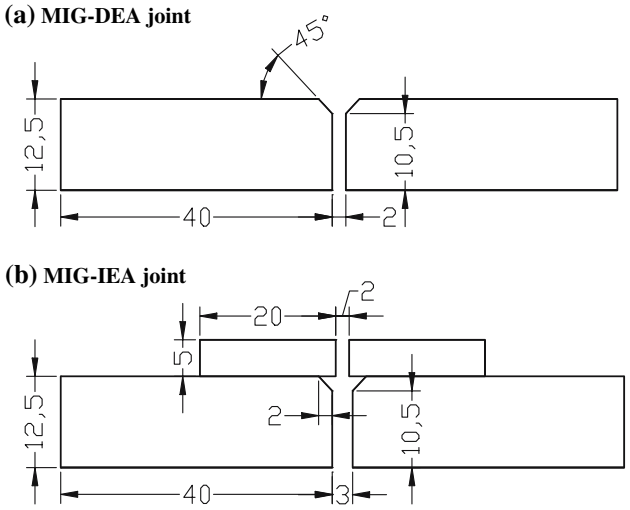

Fig. 1 Joint design and dimensions (mm) when the electric arc is applied (**a**) directly and (**b**) indirectly

Weld profiles and metallography

After welding the DEA and IEA joints, the weld beads were cross-sectioned and prepared for examination. In order to reveal the actual weld configuration, samples were ground with 240, 400 and 800 grit SiC papers, polished to a mirror-like finish using 6 and 1 μm diamond compounds and etched with a solution of 7% HF, 7% HCl, 49% HNO_3 and 37% H_2O. Disclosure of the weld profile enabled calculation of the base metal diluted by using the equation:

$$\%\text{Dilution} = \frac{F_p}{(F_g + F_r + F_p)} \times 100 \quad (1)$$

given in Ref. [12], where F_p, F_g and F_r correspond to the cross-sectional areas, as shown in Fig. 2, of base metal melted, groove and weld reinforcement, respectively. Digital images of the etched weld profiles, at natural size, along with software facilities (AutoCAD 2005) were used to replicate the initial configuration of the joints and the contour of the weld beads to finally measure the corresponding areas shown in Fig. 2.

Weld samples for metallography were also polished and anodised, to reveal the grain structure in both weld metal and HAZ, in a 2% solution of HBF_4 in water for 2 min at 16 V. The samples were then viewed in an optical microscope, coupled to a digital camera, under crossed-polars.

Thermal balance

A thermal balance of the heat inputted by the electric arc with respect to the heat consumed to melt an amount of both feed and parent metals plus the flux of heat into the parent metal was performed. The thermal balance allows comparison of the use of heat generated by the electric arc in both methods, direct and indirect, as well as to calculate the average temperature at which the molten feed material is supplied during the welding process by IEA.

The heat balance was made, considering the weld profiles, in order to quantify the heat consumed to melt a volume of material in one second, as well as to determine the heat flux into the proportional lateral area of the parent metal to then compare the result with respect to the heat supplied to the area to be welded in this time period. The volumes of metal melted (V) in one second by both DEA and IEA were determined using the total area of weld metal ($A_T = F_g + F_r + F_p$) as, $V = A_T \times 3.6$, where 3.6 is the travelling speed of the welding torch in mm/s.

Table 1 Chemical composition of the metallic materials employed (wt%)

Material	%Al	%Si	%Fe	%Cu	%Mn	%Mg	%Cr	%Ni	%Zn	%Ti
ER4043	Bal.	5.25	0.8	0.3	0.05	0.05	–	–	0.10	0.02
Al-1010	Bal.	0.2	0.65	0.005	0.002	0.014	0.012	0.009	0.002	–
Al-2024	Bal.	0.35	0.36	4.46	1.08	1.86	0.017	–	0.047	–

Table 2 Parameters employed to weld Al by the MIG welding process using DEA and IEA

Parameter	Value
Current	250 A
Voltage	22 V
Travel speed	3.6 mm/s
Argon flow rate	22 L/min
Preheating temperature	50 and 100 °C
Heat input	5.5 kJ/s
Stick out	12 mm

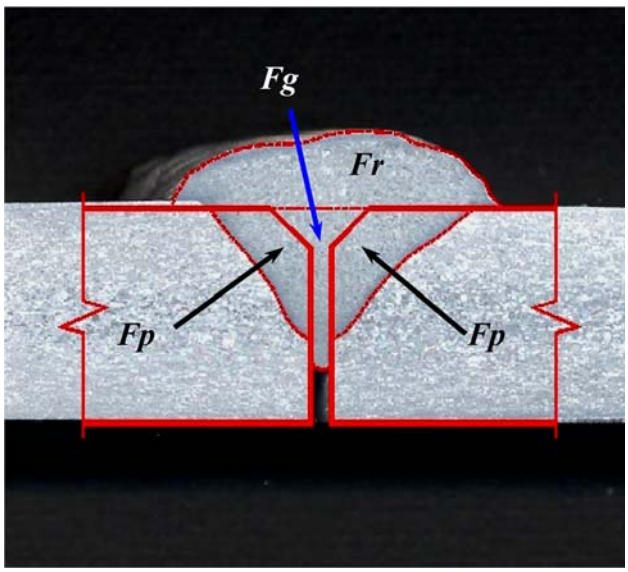

Fig. 2 Cross-sectional areas of the welded joint. F_p = base metal melted, F_g = metal filling the groove and F_r = weld reinforcement

The heat consumed (ΔH_{TF}) to melt the corresponding mass of metal in 1 s was calculated through Eq. 2 which determines the heat required to melt one mol of aluminium:

$$\Delta H_{TF} = \int_{T_{ph}}^{T_m} C_p \, dT + \Delta H_m \tag{2}$$

where C_p is specific heat of solid aluminium, ΔH_m is the latent heat of fusion of aluminium, T_{ph} is the preheating temperature and T_m is the melting point of aluminium. The fraction of Al-2024 in the weld metal was estimated to be approximately 18.13% for the MIG-IEA joint welded at 100 °C and as thermochemical parameters for aluminium alloys are hardly established [6, 7] the values for aluminium of commercial purity were employed. The flux of heat by conduction through the parent metal was calculated using Eq. 3:

$$\frac{\partial^2 T}{\partial x^2} + \frac{\partial^2 T}{\partial y^2} + \frac{\partial^2 T}{\partial z^2} = \frac{C_P}{k}\frac{\partial T}{\partial t} \tag{3}$$

where k is the thermal conductivity of Al (0.204 J/mm °C), ∂T is the temperature differential and ∂x, ∂y and ∂z are differentials of distance representing the distance travelled in 1 s by the welding torch.

In order to calculate the temperature at which the liquid metal is supplied into the butt DEA and IEA joints, Rosenthal's equation [13, 14], which considers full penetration of the weld and enables an estimation of the temperatures of the weld pool around the centre of the electric arc, was employed for two dimensions:

$$T - T_0 = \frac{q}{2\pi k\eta} e^{\left(\frac{-v}{2a}\right)(\xi + r)} \sqrt{\frac{a\pi}{vr}} \tag{4}$$

where k is thermal conductivity of Al, a is the thermal diffusivity, q is the heat flux, r is the radius in mm, η is the process efficiency, v is the travel speed of the torch, T_0 is the initial joint temperature, T is the electric arc temperature, and ξ is the relationship between the coordinates of the point under consideration along the x-axis at any time t, which can be calculated by $\xi = x - vt$.

Results

Weld beads characteristics

The cross-section of the etched welds using DEA and IEA welding procedures are shown in Figs. 3 and 4. The etching given to the samples did not disclose the HAZ but it did reveal the weld beads. Thus, it is clearly observed in Fig. 3a that there is not sufficient penetration when preheating the joint to 50 °C, while Fig. 3b shows that this problem is overcome by pre-heating the joint to 100 °C. There is, however, lack of lateral fusion in the lower part of the joint and the significant volume of base metal melted

on top of the weld bead made the welded joint very irregular. These characteristics prove the necessity of a more elaborate joint preparation. Although distortion of the welds was not evaluated, some degree of deformation can be observed in Fig 3b. On the other hand, Fig. 4 reveals the change in morphology of the weld profile when the electric arc is indirectly applied as compared to the DEA weld profiles shown in Fig. 3 for the same thickness and preheating condition. In the IEA welds there is full penetration along the height of the weld with no signs of lack of lateral fusion. Notice that the large defect present in Fig. 4b falls within the height of the feeding strips and it does not affect the integrity and strength of the welded joint. Generally speaking, experimental results show that the MIG-IEA welding process achieves larger weld penetration with weld profiles that are more uniform than those obtained by directly applying the electric arc to the aluminium plates. Typically to weld 12.5 mm thick plates, it is necessary to use a double V groove preparation with two welding passes, one in each side or alternatively a single V groove with two or more alternating welding passes. Both procedures require a greater amount of filler metal to be deposited, which leads a larger heat input and HAZ and, if care is not taken, to major distortion in the welded joint. In the welding process with IEA, deformation of the joints was minor. Further trials with a 6061-T6 alloy showed that the MIG-IEA technique also reduces the HAZ when successful joining is achieved by both techniques (R.R. Ambriz et al. submitted).

Microstructure

Figure 5 shows the grain structure of the Al-1010 plates observed along the height of the plates in a cross-section perpendicular to the welding direction. It was found that the top and bottom of the Al-1010 plates is characterised by a grain size roughly ranging between 50 to 250 μm, as observed in Fig. 5a. In the mid height of the plates, a coarser grain structure roughly varying between 50 to 400 μm is observed in Fig. 5b.

Figures 6 and 7 show the typical solidification microstructures at the fusion line for the MIG DEA and IEA joints welded at 100 °C. First of all, notice that there is not an observable grain growth in the HAZ of the base metal for both joints, although the aluminium plates were preheated, In the MIG-DEA optical micrographs, the traditional epitaxial and columnar growth from the partially melted grains of the base metal obtained by the direct application of the arc are observed, whereas the microstructure in Fig. 7 for the MIG-IEA joint, reveals features with a different solidification microstructure in which it seems that partially melted grains of base metal are trapped within the weld metal. These characteristics are more evident in Fig. 8 which shows optical micrographs of the microstructure for samples etched with Keller's reagent in the transversal (Fig. 8a) and longitudinal (Fig. 8b) axes of the weld. Notice the similar response to etching between the grains pointed in the micrographs and the base metal.

To fully ascertain whether or not these grains correspond to the base metal, samples were loaded in a scanning electron microscope (SEM). Energy dispersive X-ray (EDX) analyses and X-ray dot maps were conducted as shown in Figs. 9 and 10, respectively. EDX analyses performed on dendritic grains of the weld metal revealed, as expected, high levels of Si and the presence of Cu, where as for the suspected base metal partially melted grains within the weld the analyses gave average Si content of 0.48 wt.%. Chemical composition of the aluminium plates indicated a silicon content of 0.2 wt.%. Although the values from EDX for these grains are high, they are nevertheless, close to the base metal Si content, so that small difference can be due to some diffusion of silicon into the grains. If the evidence gained from the quantitative analyses might not be that convincing, the elemental X-ray maps shown in Fig. 9 irrefutably reveal that effectively these grains correspond to base metal partially melted grains as the grain pointed within the weld metal exhibits a distribution or intensity of silicon similar to that observed in the base metal. This evidence thus indicates that these grains corresponds to grains dragged from the base metal which only partially melted and survived in the weld metal near to the fusion line.

Thermal balance

The results obtained for the thermal balance and temperatures around the electric arc according to Rosenthal's equation are shown in Tables 3 and 4 respectively. From

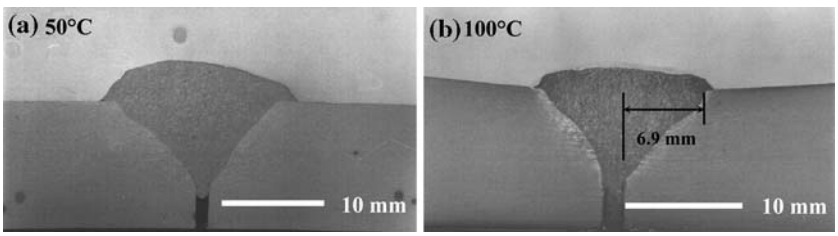

Fig. 3 Profiles of the weld beads deposited with DEA

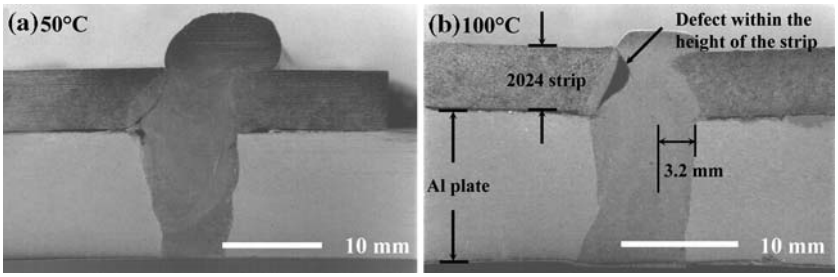

Fig. 4 Profiles of the weld beads deposited with IEA

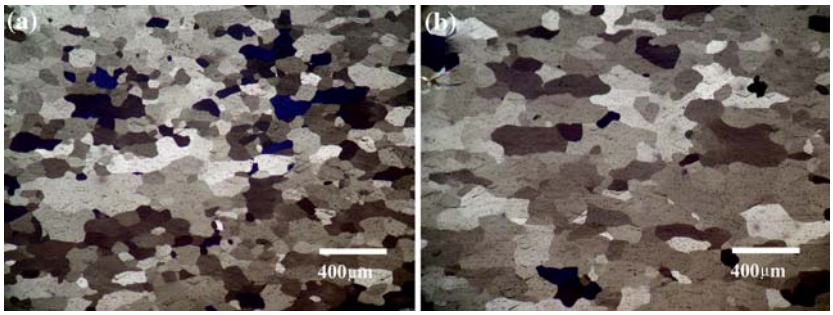

Fig. 5 Grain structures of the cross-section in the base metal corresponding to (**a**) top and (**b**) mid height

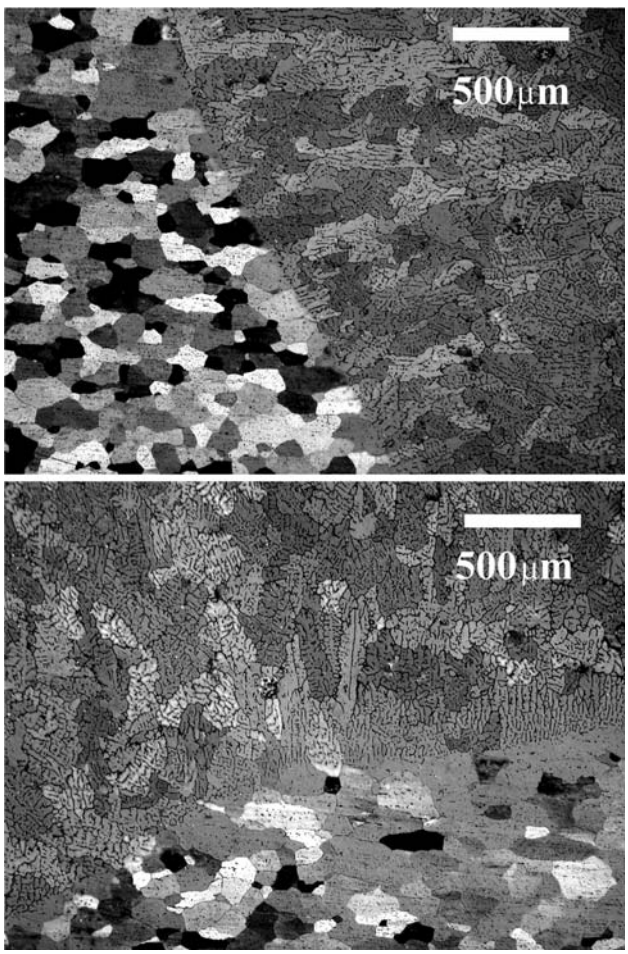

Fig. 6 Base metal/weld interfaces obtained by MIG-DEA with preheating to 100 °C

Table 3 it is observed that the MIG-IEA method yields higher efficiencies than the MIG-DEA. Estimations of the temperature in the weld pool by Rosenthal's equation for a heat moving source with the efficiencies calculated for the welds performed in this study, Table 4, indicate that while the temperatures in the proximity of the electric arc are significantly higher for the MIG-IEA joints, the difference is basically null between joints irrespective of preheating temperatures for a distance of 4.5 mm.

Discussion

The results, obtained under the experimental conditions and with the novel configuration of the joint, have shown that the MIG-IEA welding process is a viable joining method which improves the morphology of the transverse section of the welds, in contrast with the typical profiles obtained by the welding process in which the electric arc is directly applied. High penetration, a uniform cross configuration of the weld and increased lateral fusion along the height of the parent metal are typical characteristics obtained by this technique. These features are achieved by virtue of a better use of the energy developed by the electric arc over the parent metal as the success of the welding operation also depends on the heat input to the joint and how much of it is efficiently used. The thermal balance showed that approximately 90–95% of the energy developed by the electric arc is consumed during fusion of electrode, feeding strips and parent metal. This efficiency is greater than when the electric arc is directly applied. In addition to the characteristics highlighted, the feed material

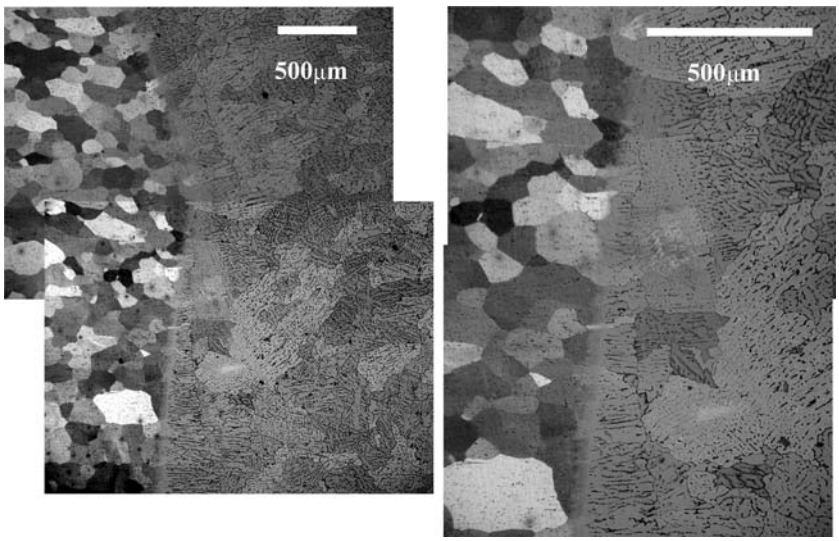

Fig. 7 Base metal/weld interfaces obtained by MIG-IEA with preheating to 100 °C

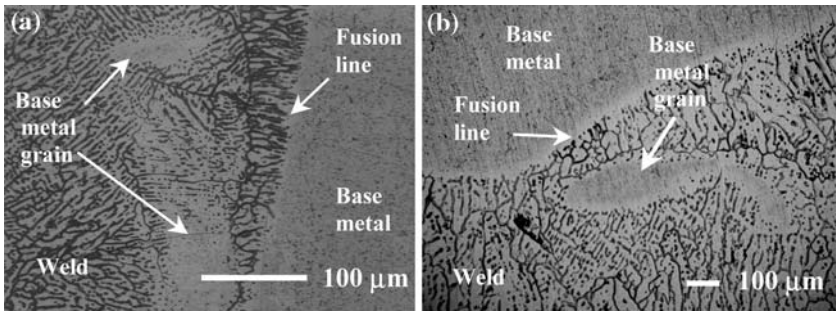

Fig. 8 Optical micrographs of the base metal/weld interface: (**a**) in the transversal and (**b**) longitudinal axes of a MIG-IEA weld

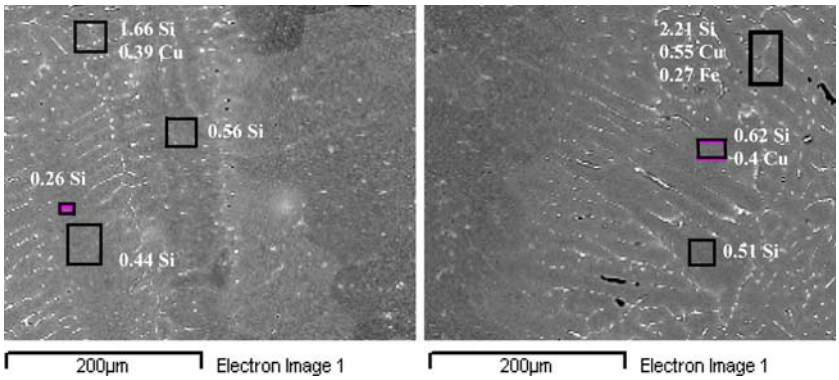

Fig. 9 Base metal/weld interfaces of a MIG-IEA welded joint with data of the chemical composition obtained by EDX analysis

may be selected with equal or greater strength than the parent metal and, based on the reduced thermal affection of the parent metal welded in a single pass instead of two or three, cracking susceptibility in some materials may be alleviated through the use of the proposed MIG-IEA technique.

Predictions by Rosenthal's equation show that the temperatures around the electric arc are higher as the preheating temperature increases but also, temperatures for the IEA process are significantly higher than those predicted for DEA. Besides, these temperatures at different distances from the centre of the electric arc agree well with the profile of the weld beads. For example in the IEA samples, Rosenthal's equation predicts a temperature of approximately 655 °C at a distance of 4.5 mm which is closely matching with the weld contour of the profile. In contrast, predictions fail to estimate the width of the weld with regard to the temperatures reached around the electric arc for the DEA joint. This is because for DEA welds the condition of full penetration is not met and the heat provided is concentrated on top of the joint widening thus the top of the weld bead.

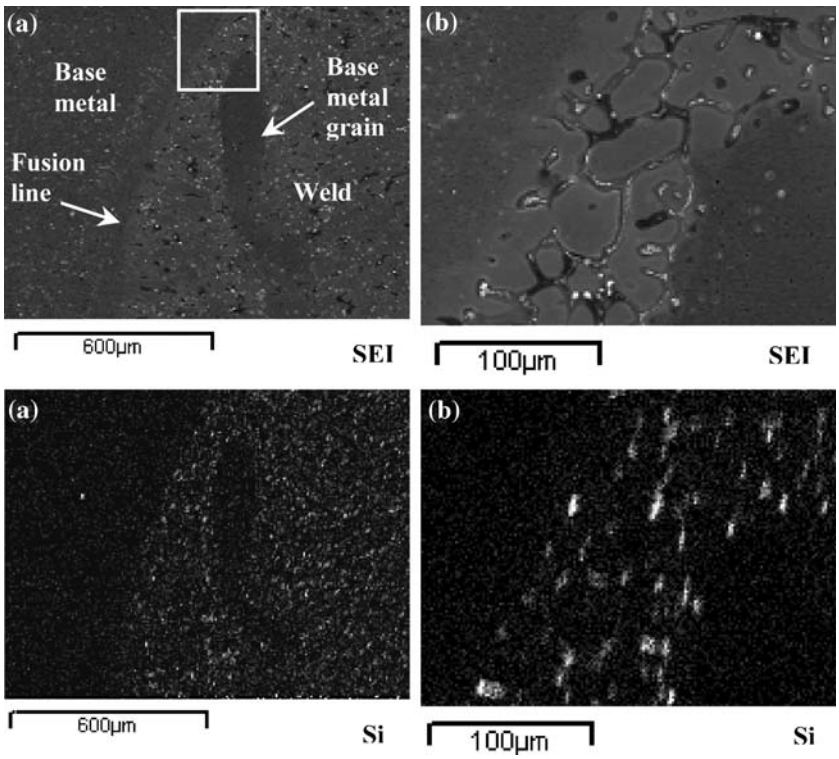

Fig. 10 Elemental X-ray mapping showing the distribution of silicon for: (**a**) the region shown in Fig. 8b and (**b**) enlargement corresponding to the *square* in Fig. 10a

Table 3 Summary of the thermal balance for the MIG process using DEA and IEA

Variable	DEA		IEA	
Preheating temperature (T_{ph})	50 °C	100 °C	50 °C	100 °C
F_p (mm^2)	60.88	59.13	71.72	92.35
Transversal area (A_T, mm^2)	119.95	118.20	130.79	151.41
Volume melted (V, mm^3/s)	431.82	425.54	470.87	545.09
Weight of metal melted (g)	1.1659	1.2213	1.27	1.47
ΔH of fusion (ΔH_{TF}, kJ)	1.2393	1.2213	1.3514	1.5643
ΔH conduction (q_x, kJ)	3.061	3.242	3.494	3.649
ΔH total heat supplied to the parent metal (ΔH_T, kJ)	4.3003	4.4633	4.8454	5.2176
%Dilution	53	46	32	46.5
Supplying average temperature of liquid metal	–	–	1930 °C	2150 °C
Efficiency (%)	78.187	81.15	88.09	94.8

Table 4 Temperatures around the electric arc according to Rosenthal's equation

Radius (r)	DEA, 50 °C	DEA, 100 °C	IEA, 50 °C	IEA, 100 °C
1.0 mm	1993 °C	2120 °C	2372 °C	2498 °C
1.5 mm	1614 °C	1715 °C	1916 °C	2017 °C
4.5 mm	652 °C	654 °C	655 °C	656 °C

Calculations of the temperature of liquid metal indicate temperatures of approximately 1,930 and 2,150 °C for MIG-IEA joints preheated to 50 and 100 °C, respectively. These temperatures seem to be reasonable as experimental studies performed by Lou and Kou [6, 7] showed that for a spray transfer mechanism, which is dictated by the welding parameters of voltage and current, the liquid droplets of the electrode are transferred at 2,200 °C. The higher temperatures in the supply of liquid metal for IEA welds enable major penetration as well as good lateral fusion of the base

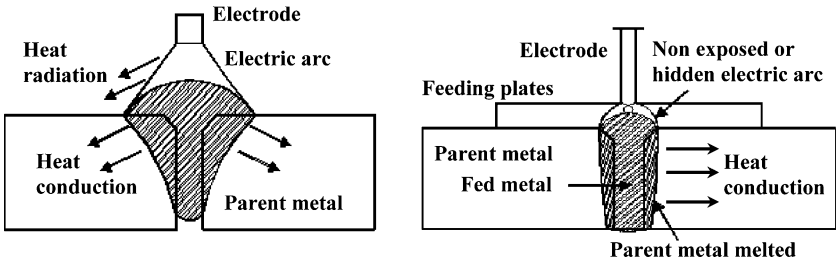

Fig. 11 Establishment of the electric arc in open and hidden modes by (**a**) MIG-DEA and (**b**) MIG-IEA, respectively

metal owing to the reduction of heat losses. Another feature of the MIG-IEA process, which explains the above statement and the increase in the thermal efficiency, is the fact that the electric arc established is not exposed to the atmosphere as in the DEA technique; instead it is established in a hidden fashion within the feed metal strips as depicted in Fig. 11. This is mainly due to the low ionization potential of the aluminium vapour, 5.986 eV [1].

The losses of the electric arc as a percentage of the thermal energy by radiation and convection, can be calculated by the equation developed by Dupont [2]:

$$E_{\text{arc}} + \text{electrode} = E_{\text{lost}} + E_{\text{zf}} + E_{\text{mb}} \quad (5)$$

where the terms on the left-hand side of the equation represent the energy developed by the electric arc and the electrode, whereas the terms on the right side are the total energy losses by radiation and convection, the energy consumed by fusion and conduction, respectively.

In this work the energy lost by radiation and convection is minimized since the electric arc is generated in a hidden form (Fig. 11b), instead of being openly exposed to the atmosphere as typically occurs in DEA (Fig. 11a). Therefore Eq. 5 can be written as

$$E_{\text{arc}} + \text{electrode} = E_{\text{minimum lost}} + E_{\text{zf}} + E_{\text{mb}} \quad (6)$$

Regarding the microstructure, for the MIG-DEA joint the typical epitaxial and columnar dendritic growth was observed whilst the IEA weld does not consistently exhibit this characteristic. Instead, the growth is restricted and there are some grains of base metal trapped within the weld metal. These trapped grains were present along the height of the weld next to the fusion line. It is thought that fusion of the base metal grain boundaries occurs preferentially, although the precise mechanism of partial fusion of grains in the base metal leaving some of them trapped within the weld metal close to the fusion line is not clear.

Conclusions

The MIG welding process using IEA emerges as an adequate route to modify the profile of the weld bead yielding welds with high depth-to-width ratios. Since the defects of the weld deposits by IEA are located outside of the weld bead in the upper part, sound welds may be obtained by this modified MIG welding process. The improvement of the efficiency of the MIG welding process up to 94.8% using IEA may be ascribed to the better use of heat generated by the electric arc, which is established in a hidden form and the contact with the environment is minimum reducing thus heat losses.

Acknowledgements The authors would like to thank Coordinación de la Investigación Científica of the UMSNH for funding this study and to Dra. Lourdes Mondragón from Instituto Tecnologico de Morelia for the facilities consented in the use of the SEM.

References

1. American Welding Society (1976) Welding handbook, 7th edn, vol 1. American Welding Society, p 71
2. Dupont JN, Murder AR (1995) Weld J 74:406
3. Furschbach PW, Knorovsky GA (1991) Weld J 70:287
4. Choo RT, Szekely J, Westhoff RC (1990) Weld J 60:346
5. Kim YS, Mceligot DM, Wagar TW (1991) Weld J 70:20
6. Lu MJ, Kou S (1989) Weld J 68:382
7. Lu MJ, Kou S (1989) Weld J 68:452
8. Kim JW, Na SJ (1995) Weld J 74:141
9. Cao ZN, Dong P (1998) ASME J Eng Mater Tech 120:313
10. Garcia R, Lopez VH, Bedolla E, Manzano A (2000) J Mater Sci Lett 21:1965
11. Garcia R, Lopez VH, Bedolla E, Manzano A (2003) J Mater Sci 38:2771
12. Malin V (1995) Weld J 74:305-s
13. Rosenthal D (1946) Trans ASME 68:849
14. Christensen N, de Davies VL, Gjermundsen K (1965) Br Weld J 12:54